

Smearing technique for vibration analysis of simply supported cross-stiffened and doubly curved thin rectangular shells^{a)}

Yu Luan^{b)}

Acoustic Department, Bang & Olufsen, Peter Bangs Vej 15, DK-7600, Struer, Denmark

Mogens Ohlrich and Finn Jacobsen

Acoustic Technology, Department of Electrical Engineering, Technical University of Denmark, Building 352, DK-2800 Kongens Lyngby, Denmark

(Received 13 November 2009; revised 28 October 2010; accepted 7 November 2010)

Plates stiffened with ribs can be modeled as equivalent homogeneous isotropic or orthotropic plates. Modeling such an equivalent *smear*ed plate numerically, say, with the finite element method requires far less computer resources than modeling the complete stiffened plate. This may be important when a number of stiffened plates are combined in a complicated assembly composed of many plate panels. However, whereas the equivalent smeared plate technique is well established and recently improved for flat panels, there is no similar established technique for doubly curved stiffened shells. In this paper the improved smeared plate technique is combined with the equation of motion for a doubly curved thin rectangular shell, and a solution is offered for using the smearing technique for stiffened shell structures. The developed prediction technique is validated by comparing natural frequencies and mode shapes as well as forced responses from simulations based on the smeared theory with results from experiments with a doubly curved cross-stiffened shell. Moreover, natural frequencies of cross-stiffened panels determined by finite element simulations that include the exact cross-sectional geometries of panels with cross-stiffeners are compared with predictions based on the smeared theory for a range of different panel curvatures. Good agreement is found.

© 2011 Acoustical Society of America. [DOI: 10.1121/1.3523305]

PACS number(s): 43.40.Ey, 43.40.Dx [JHG]

Pages: 707–716

I. INTRODUCTION

Stiffeners are efficient for enhancing the stiffness of a plate or shell structure without adding unnecessary amounts of mass as a simple increase of plate thickness would do. However, the increased complexity of plates with added stiffeners normally requires much longer computing time for finding the structural acoustic properties of a stiffened structure in a design process. To reduce the computational effort, a coarse but efficient method is to *smear* the stiffeners to the base plate or shell. This technique of smeared stiffened plates with an effective torsional rigidity was developed by Lampert in the 1970s¹ and summarized by Szilard in 2004.² The accuracy of this technique for flat plates has recently been improved.³ However, there is no similar established theory for doubly curved stiffened shells, and this is the subject of the present paper.

In the last 40 years researchers have paid a great deal of attention to the dynamic behavior of stiffened shells. Works have been done on cylindrical shells^{4–29} and on conical shells.^{30,31} Since doubly curved shells need more degrees of freedom for analysis researchers mostly use the finite element method (FEM) to deal with such cases. The application

of FEM to the vibration analysis of a stiffened shell makes it possible to model discrete stiffeners, variable curvature, and irregular geometry. However, FEM calculations based on the detailed geometries of such panels have been found to be very time-consuming.

Nowadays, engineers usually draw a new design structure with a three-dimensional program and later simulate its dynamic properties with an FEM program. The drawing process and the FEM calculations may take days or even weeks for a relatively simple structure. Furthermore, it is often necessary to make modifications to the structure and for that new FEM calculations are required. All this can be very time-consuming. Even though computers become more and more powerful, the engineer's working hours for making a drawing and developing an FEM model have almost not changed. Thus, it is very useful if the geometry can be simplified, for example, by the smearing technique.

The purpose of this paper is to present a smearing technique for determining the natural frequencies and mode shapes of a simply supported doubly curved thin rectangular shell with periodically arranged small stiffeners. The smearing technique becomes unreliable at high frequencies, where half of the bending wavelength in the base plate becomes comparable to—or smaller than—the stiffener spacing. However, the proposed technique is useful for making a fast estimate, although its application is limited to the lower number of vibrational modes.

The expressions to be derived in the following for stiffened shells are based fundamentally on smeared properties of

^{a)}Portions of this work were presented in "The structural acoustic properties of stiffened shells," Proceedings of Acoustics'08, Paris, France, 2008.

^{b)}Author to whom correspondence should be addressed. Current address: Acoustic Technology, Department of Electrical Engineering, Technical University of Denmark. Electronic mail: yl@elektro.dtu.dk

equivalent flat plates with stiffeners. Such properties of flat stiffened plates are therefore summarized in Sec. II. These results are then utilized, in Sec. III, for developing the smearing technique for curved cross-stiffened panels. In Sec. IV predictions using the developed smearing technique are validated experimentally for a weakly doubly curved and cross-stiffened panel. It is demonstrated that good agreement is achieved between predicted and measured values of natural frequencies and mode shapes as well as forced responses in terms of point and transfer mobilities. With the smearing technique experimentally validated for the test panel, this technique is then used for predicting the modal properties of cross-stiffened panels for a range of different curvatures. These predicted results are compared with finite element (FE) calculations (using ANSYS) in which all stiffener details are modeled; these time-extensive FE calculations are used as reference for evaluating the predicted results.

II. SMEARED STIFFENED PLATE

It has long been recognized that the lower modes of vibration of stiffened plates may be estimated by “smearing” the mass and stiffening effects of the stiffeners over the surface of the plate. The results in this section are based on existing theory.^{2,3}

In the following, the natural frequencies of a thin rectangular plate with cross-stiffeners are determined. The plate is simply supported along all four edges. The geometrical parameters of the plate are shown in Fig. 1; the length of the plate is a in the x direction and b in the y direction, and its

thickness is h . The stiffeners in the x direction have the width w_{sx} , height h_{sx} , and spacing b_s and in the y direction the corresponding values are w_{sy} , h_{sy} , and a_s .

The governing equation of motion for an equivalent smeared plate of the stiffened plate has been derived by Szilard;² for the transverse displacement $w(x, y, t)$ this yields

$$D_x \frac{\partial^4 w(x, y, t)}{\partial x^4} + 2H \frac{\partial^4 w(x, y, t)}{\partial x^2 \partial y^2} + D_y \frac{\partial^4 w(x, y, t)}{\partial y^4} + \rho h_e \frac{\partial^2 w(x, y, t)}{\partial t^2} = p, \quad (1)$$

where D_x and D_y are the equivalent bending stiffness per unit width in the x and y directions, H is the effective torsional rigidity, ρ is the mass density of the material, h_e is the thickness of the equivalent smeared plate, and p is the external forcing. The development of the improved D_x and D_y can be found in Ref. 3, but for ease of reference some details are also given in the Appendix. With the stiffeners smeared and spread on top of the plate, the thickness of the equivalent smeared plate becomes

$$h_e = h + h_s w_s \left(\frac{1}{a_s} + \frac{1}{b_s} \right) - \frac{h_s w_s^2}{a_s b_s}. \quad (2)$$

For a thin cross-stiffened rectangular plate with all edges simply supported, the natural frequencies of the corresponding smeared plate are³²

$$f_{mn, \text{flat, stiff}} = \frac{1}{2\pi} \sqrt{\frac{1}{\rho''} \sqrt{D_x \left(\frac{m\pi}{a} \right)^4 + 2H \left(\frac{m\pi}{a} \right)^2 \left(\frac{n\pi}{b} \right)^2 + D_y \left(\frac{n\pi}{b} \right)^4}}, \quad (3)$$

where $\rho'' = \rho h_e$ is the smeared average mass per unit area, and the integers m and n are the mode numbers corresponding to the x and y directions.

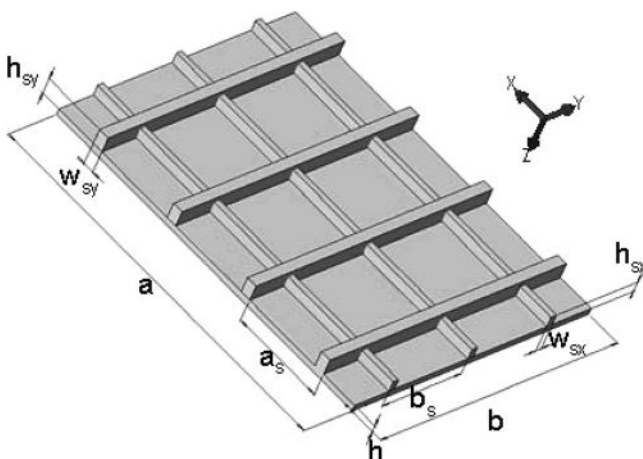


FIG. 1. Geometrical parameters of a cross-stiffened flat rectangular plate.

III. SMEARED STIFFENED SHELL

In this section, an equation for the natural frequencies of a simply supported doubly curved and cross-stiffened rectangular shell is presented together with an expression for the forced response. First, the unstiffened rectangular shell is considered.

A. Natural frequencies of a doubly curved thin rectangular shell

Soedel studied a simply supported doubly curved rectangular shell.³³ Here, the shell has a constant radius of curvature R_x in the x direction, and a constant radius of curvature R_y in the y direction. The x - y coordinate system is selected on the imagined flat base plate. The curved edge lengths of the shell are a in the x - z plane, and b in the y - z plane, and the thickness of the shell is h . In what follows E is the Young's modulus, ν is the Poisson's ratio, and ρ is the density.

Assumptions such as Donell–Mushtari–Vlasov's simplification and the infinitesimal distance assumption are used in

Soedel's derivation. The first basic assumption of Donell–Mushtari–Vlasor's simplification is that contributions of in-plane deflections can be neglected in the bending strain expressions but not in the membrane strain expressions. The second assumption is that the influence of inertia in the in-plane direction can be neglected. Third, the infinitesimal distance assumption is

$$(ds)^2 \cong (dx)^2 + (dy)^2, \quad (4)$$

where ds is the magnitude of the differential change.³³ Both assumptions introduce a considerable error in the estimation of the fundamental natural frequency.¹¹

With these assumptions, the equation of motion for free transverse vibration $w(x, y, t) = U_3 e^{i\omega t}$ of a homogenous shell becomes³³

$$D\nabla^8 U_3 + Eh\nabla_k^4 U_3 - \rho''\omega^2\nabla^4 U_3 = 0, \quad (5)$$

where

$$D = \frac{Eh^3}{12(1-\nu^2)}, \quad (6)$$

$$\nabla^2(\cdot) = \frac{\partial^2(\cdot)}{\partial x^2} + \frac{\partial^2(\cdot)}{\partial y^2}, \quad (7)$$

$$\nabla_k^2(\cdot) = \frac{1}{R_x} \frac{\partial^2(\cdot)}{\partial x^2} + \frac{1}{R_y} \frac{\partial^2(\cdot)}{\partial y^2}, \quad (8)$$

in which $\rho'' = \rho h$ is the mass per unit area, and D is the bending stiffness. For the doubly curved, simply supported rectangular shell, the transverse displacement is expressed by a double sine series with terms of the form

$$U_{3,mn} = A_{mn} \sin \frac{m\pi x}{a} \sin \frac{n\pi y}{b}. \quad (9)$$

Substituting Eq. (9) into Eq. (5) gives

$$D \left[\left(\frac{m\pi}{a} \right)^2 + \left(\frac{n\pi}{b} \right)^2 \right]^4 + Eh \left[\frac{1}{R_x} \left(\frac{m\pi}{a} \right)^2 + \frac{1}{R_y} \left(\frac{n\pi}{b} \right)^2 \right]^2 - \rho''\omega^2 \left[\left(\frac{m\pi}{a} \right)^2 + \left(\frac{n\pi}{b} \right)^2 \right]^2 = 0. \quad (10)$$

The natural frequencies are therefore

$$f_{mn,curve}^2 = \frac{1}{4\pi^2} \left[\left(\frac{m\pi}{a} \right)^2 + \left(\frac{n\pi}{b} \right)^2 \right]^2 \frac{D}{\rho''} + \frac{\left[\frac{1}{R_x} \left(\frac{m\pi}{a} \right)^2 + \frac{1}{R_y} \left(\frac{n\pi}{b} \right)^2 \right]^2}{4\pi^2 \left[\left(\frac{m\pi}{a} \right)^2 + \left(\frac{n\pi}{b} \right)^2 \right]^2} \cdot \frac{E}{\rho}. \quad (11)$$

It is well known that the natural frequencies of a thin rectangular flat plate are

$$f_{mn,flat} = \frac{1}{2\pi} \sqrt{\left[\left(\frac{m\pi}{a} \right)^2 + \left(\frac{n\pi}{b} \right)^2 \right]^2 \frac{D}{\rho''}} \\ \Rightarrow f_{mn,flat}^2 = \frac{1}{4\pi^2} \left[\left(\frac{m\pi}{a} \right)^2 + \left(\frac{n\pi}{b} \right)^2 \right]^2 \frac{D}{\rho''}, \quad (12)$$

where the geometrical and material parameters of the flat plate are the same as those of the curved shell except for the curvatures. Therefore, Eq. (11) can be rewritten,

$$f_{mn,curve}^2 = f_{mn,flat}^2 + \frac{\left[\frac{1}{R_x} \left(\frac{m\pi}{a} \right)^2 + \frac{1}{R_y} \left(\frac{n\pi}{b} \right)^2 \right]^2}{4\pi^2 \left[\left(\frac{m\pi}{a} \right)^2 + \left(\frac{n\pi}{b} \right)^2 \right]^2} \cdot \frac{E}{\rho}. \quad (13)$$

All in all, the formula for the natural frequencies of a simply supported, doubly curved, thin rectangular shell can be seen to be the sum of two terms. The first term relates to a flat plate that has the same geometrical and material parameters as the curved shell except for the curvatures; the second term is accounting for the curvature. In other words, in parts a doubly curved rectangular shell has properties similar to a flat rectangular plate for which the shell is pressed and extended into a flat surface. The thickness does not change during this process. The edge lengths of the flat plate are equal to the curved edge lengths of the shell, which are still a and b . Thus, the natural frequencies of the doubly curved shell can be obtained by finding the natural frequencies of the related flat plate and adding the curvature term; see Eq. (13).

B. Natural frequencies of a simply supported, doubly curved, and cross-stiffened thin rectangular shell

This section presents the natural frequencies of a simply supported, doubly curved, and cross-stiffened thin rectangular shell. Both a physical explanation and an analytical derivation are offered.

Equation (13) indicates a possible way of finding the natural frequencies even for a doubly curved *cross-stiffened* shell. If these stiffeners are smeared on the surface of the shell, the resulting structure can be regarded as an equivalent smeared shell. The smeared shell also has its related plate, which is the shell pressed and extended into a flat surface. The related smeared plate has its equivalent bending stiffness in the x and y direction, D_x and D_y , torsional rigidity, H , and equivalent thickness, h_e . None of these parameters appears in the curvature term in Eq. (13), which means that this term is independent of the smearing technique. The two terms in Eq. (13) can thus be obtained individually. Equation (3) yields the natural frequencies of the related plate, whereas the curvature term of Eq. (13) can be obtained from the base shell properties. Following these arguments this results in the natural frequencies of a simply supported, doubly curved, and cross-stiffened thin rectangular shell

$$f_{mn,curve,stiff}^2 = f_{mn,flat,stiff}^2 + \frac{\left[\frac{1}{R_x} \left(\frac{m\pi}{a} \right)^2 + \frac{1}{R_y} \left(\frac{n\pi}{b} \right)^2 \right]^2}{4\pi^2 \left[\left(\frac{m\pi}{a} \right)^2 + \left(\frac{n\pi}{b} \right)^2 \right]^2} \cdot \frac{E}{\rho}. \quad (14)$$

An analytical derivation of Eq. (14) can be developed by using the equation of motion for the shell. Equation (5) can represent an equation of motion for a stiffened shell, provided that the parameters D , h , and $\rho'' = \rho h$ are replaced by the corresponding properties of an equivalent smeared shell, that is, by D_e , h_e , and $\rho'' = \rho h_e$. The equation of motion of the equivalent smeared shell therefore becomes

$$D_e \nabla^8 U_3 + E h_e \nabla_k^4 U_3 - \rho'' \omega^2 \nabla^4 U_3 = 0, \quad (15)$$

As can be seen from Eq. (6), the bending stiffness D of a shell is independent of the curvature. Therefore D can be obtained from a structure where the radii of the shell go to infinity, in other words, a corresponding flat plate. Similarly, the equivalent bending stiffness D_e can also be calculated for an equivalent smeared flat plate, which is the smeared shell pressed and extended into a flat surface.

It was shown in Sec. II that the equivalent smeared plate has its equivalent bending stiffnesses D_x and D_y and torsional rigidity H . In order to use Eq. (15), D_x , D_y , and H should be combined into one parameter, D_e . The challenge now is to find an expression for D_e , which should include the orthotropic behavior of the equivalent smeared plate.

It can be assumed that an equivalent “isotropic” plate, which has the same geometrical properties of the previous equivalent smeared plate, exists. Also, the “isotropic” plate has an equivalent bending stiffness, D_e , and its mechanical properties are the same as those of the mentioned equivalent smeared plate. The equation of motion of an isotropic plate is³³

$$D \left(\frac{\partial^4 w(x, y, t)}{\partial x^4} + 2 \frac{\partial^4 w(x, y, t)}{\partial x^2 \partial y^2} + \frac{\partial^4 w(x, y, t)}{\partial y^4} \right) + \rho h \frac{\partial^2 w(x, y, t)}{\partial t^2} = p. \quad (16)$$

By replacing D with D_e and h with h_e , one can use Eq. (16) as the equation of motion for the equivalent “isotropic” plate. With the simply supported boundary condition, the natural frequencies of this plate can now be obtained,

$$f_{mn, \text{iso}} = \frac{1}{2\pi} \left[\left(\frac{m\pi}{a} \right)^2 + \left(\frac{n\pi}{b} \right)^2 \right] \sqrt{\frac{D_e}{\rho h_e}}. \quad (17)$$

Since the “isotropic” plate has the same mechanical properties as the equivalent smeared plate, their natural frequencies should also be identical. They are

$$f_{mn, \text{iso}} = f_{mn, \text{flat, stiff}}. \quad (18)$$

Substituting Eqs. (3) and (17) into Eq. (18) gives an expression for the bending stiffness of the assumed “isotropic” equivalent plate,

$$D_e = \frac{D_x \left(\frac{m\pi}{a} \right)^4 + 2H \left(\frac{m\pi}{a} \right)^2 \left(\frac{n\pi}{b} \right)^2 + D_y \left(\frac{n\pi}{b} \right)^4}{\left[\left(\frac{m\pi}{a} \right)^2 + \left(\frac{n\pi}{b} \right)^2 \right]}. \quad (19)$$

This yields the wanted bending stiffness. Now, by substituting Eq. (19) into Eq. (15), one can obtain the natural frequencies of the simply supported, doubly curved, and cross-stiffened thin rectangular shell,

$$f_{mn, \text{curve, stiff}}^2 = \frac{1}{4\pi^2} \frac{1}{\rho''} \left[D_x \left(\frac{m\pi}{a} \right)^4 + 2H \left(\frac{m\pi}{a} \right)^2 \left(\frac{n\pi}{b} \right)^2 + D_y \left(\frac{n\pi}{b} \right)^4 \right] + \frac{\left[\frac{1}{R_x} \left(\frac{m\pi}{a} \right)^2 + \frac{1}{R_y} \left(\frac{n\pi}{b} \right)^2 \right]^2}{4\pi^2 \left[\left(\frac{m\pi}{a} \right)^2 + \left(\frac{n\pi}{b} \right)^2 \right]^2} \cdot \frac{E}{\rho}. \quad (20)$$

Note that the first term equals $f_{mn, \text{flat, stiff}}^2$ in Eq. (3). It can therefore be seen that Eq. (20) is identical with Eq. (14).

C. Forced vibration of a simply supported, doubly curved, and cross-stiffened thin rectangular shell

The smearing technique can also be used for evaluation of forced vibration of a simply supported, doubly curved, and cross-stiffened thin rectangular shell. If a pressure $p = p(x, y)$ is applied on the panel in its normal direction, it can be inserted in Eq. (15), and with Eq. (19) also substituted, the equation of motion becomes

$$D_e \nabla^8 U_3 + E h_e \nabla_k^4 U_3 - \rho'' \omega^2 \nabla^4 U_3 = \nabla^4 p, \quad (21)$$

where the pressure can be expressed by a double sine series with terms of the form

$$p_{mn} = P_{mn} \sin \frac{m\pi x}{a} \sin \frac{n\pi y}{b}. \quad (22)$$

By substituting Eqs. (9) and (22) into Eq. (21), the total displacement at position (x, y) can be found after some algebra to be

$$U_3(x, y) = \sum_{m=0}^{\infty} \sum_{n=0}^{\infty} A_{mn} \sin \frac{m\pi x}{a} \sin \frac{n\pi y}{b}, \quad (23)$$

where

$$A_{mn} = P_{mn} \frac{\left[\left(\frac{m\pi}{a} \right)^2 + \left(\frac{n\pi}{b} \right)^2 \right]^2}{D_e \left[\left(\frac{m\pi}{a} \right)^2 + \left(\frac{n\pi}{b} \right)^2 \right]^4 + E h_e \left[\frac{1}{R_x} \left(\frac{m\pi}{a} \right)^2 + \frac{1}{R_y} \left(\frac{n\pi}{b} \right)^2 \right]^2 - \rho h_e \omega^2 \left[\left(\frac{m\pi}{a} \right)^2 + \left(\frac{n\pi}{b} \right)^2 \right]^2}. \quad (24)$$

For point force excitation of amplitude F_0 at panel position (x_0, y_0) it follows that $P_{mn} = F_0 \delta(x - x_0) \cdot \delta(y - y_0)$, where δ is the Dirac delta function. The transfer mobility $Y(x, y; x_0, y_0)$ that relates the transverse velocity response at location (x, y) to a point force at (x_0, y_0) can therefore be determined from

$$Y(x, y; x_0, y_0) = \frac{i\omega U_3(x, y)}{F_0}. \quad (25)$$

The point (or direct) mobility is obtained simply by replacing the response location (x, y) by (x_0, y_0) in Eq. (25).

IV. COMPARISON OF RESULTS

A. Experiments with a curved stiffened panel

A physical model has been used to test the equation obtained by the presented smearing technique. The model is a doubly curved cross-stiffened thin rectangular shell, which is fabricated (milled out) from a solid block of polyvinyl chloride (PVC). The experimental arrangement is shown in Fig. 2, where it is seen that the solid edge block of the machined panel is screwed into a thick-walled hard-wood box, which is bolted to a 300 kg steel stand. The simply supported boundary condition of the panel was attempted accomplished by a machined narrow groove around the panel perimeter, see Fig. 2. This means that the panel was supported by a thin narrow strip that is connected to an almost rigid supporting edge. The material properties are $E = 3 \times 10^9 \text{ N/m}^2$, $\nu = 0.33$, and $\rho = 1360 \text{ kg/m}^3$. The dimensions of the shell are $a = 344 \text{ mm}$, $b = 258 \text{ mm}$, $h = 6 \text{ mm}$, $R_x = 2 \text{ m}$, and $R_y = 1.5 \text{ m}$. The pattern of the cross-stiffening is chosen to be spatially periodic, such that $a_s = 86 \text{ mm}$ and $b_s = 86 \text{ mm}$. With half end-spacing it follows that there are three stiffeners in the x direction and four stiffeners in the y direction. Stiffeners in

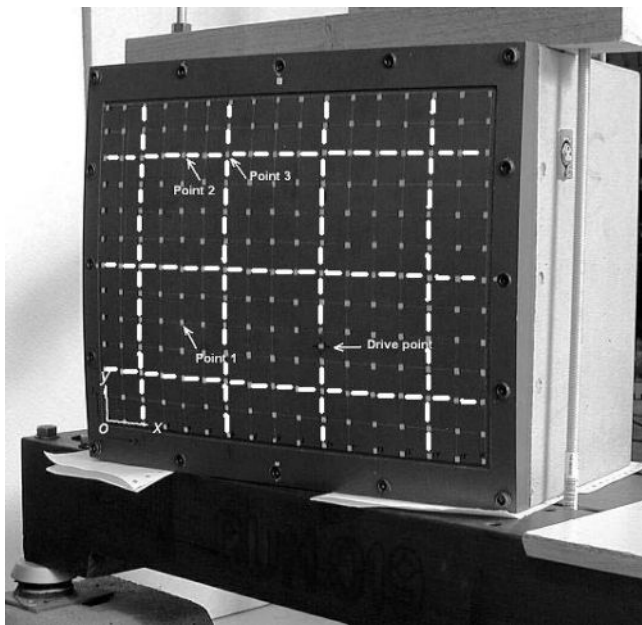


FIG. 2. Experimental arrangement with a doubly curved cross-stiffened panel. White dashed lines on the panel face show the positions of the hidden stiffeners on the rear side.

both the x and y directions had the same height, $h_{sx} = h_{sy} = 10 \text{ mm}$, and same width, $w_{sx} = w_{sy} = 6 \text{ mm}$.

The curved cross-stiffened panel was driven via a stringer at a stiffener by an electrodynamic exciter of type Brüel & Kjær (B&K, Nærum, Denmark) 4810; the coordinates of the drive point were $(x_0, y_0) = (0.213, 0.076)$, where the origin of the coordinate system is at the lower left-hand corner of the curved panel in Fig. 2. The input force was measured with a force transducer of type B&K 8200, and the response velocities were measured with a laser vibrometer of type Polytec (Waldbronn, Germany) PDV-100 at 192 points evenly spread over the panel. The force and velocity signals were fed to charge amplifiers of type B&K Nexus 2692, and the frequency response functions between velocities and excitation force were measured using a B&K “PULSE” Analyzer 3560 with a frequency resolution of 0.25 Hz.

The natural frequencies and mode shapes of the panel were obtained from the measured mobilities. In Table I the natural frequencies predicted by Eq. (20) are compared with the experimentally measured data. The mode numbers are defined as m in the x direction and n in the y direction. In the table the deviation of natural frequency denotes the difference between the predicted analytical natural frequency ($f_{\text{analytical}}$) and the experimental data (f_{Ex}). Thus, this deviation in percentage is calculated as $100 \cdot (f_{\text{analytical}} - f_{\text{Ex}}) / f_{\text{Ex}}$. Generally a very good agreement is found with deviations within 4%, except for the fundamental natural frequency; this was found to deviate from the measured value by -7% , but this mode is left out of the table. The reason for this difficulty in accurately predicting the fundamental frequency is the assumptions used in the equation of motion of the shell, Eq. (5); these assumptions introduce a considerable error in the estimation of the fundamental natural frequency.³⁴ Such deviation for the fundamental natural frequency can be up to -30% if the panel is strongly curved as is the case for some of the simulated cases that will be shown in Sec. IV B. With the chosen dimensions of the stiffened panel the range of modes (m, n) is limited to mode (3, 2) for the case considered, because the smearing method is not expected to work well when the frequency becomes so high that the spacing between the stiffeners is comparable to—or larger than—half a flexural wavelength in the base plate.

The mobilities of the panel are predicted from Eq. (25), where the numerator is obtained as the product of $i\omega$ and the displacement U_3 , which is given by Eq. (23). The damping value used in the predictions is taken to be the average value

TABLE I. Predicted and measured natural frequencies for the experimental panel model. The deviation for each mode is calculated as the difference between the analytical natural frequency ($f_{\text{analytical}}$) and the experimental data (f_{Ex}). Thus, the deviations are calculated as $100 \cdot (f_{\text{analytical}} - f_{\text{Ex}}) / f_{\text{Ex}}$.

m	N	Experiment frequency (Hz)	Analysis frequency (Hz)	Deviation (%)
2	1	327	329	0.6
1	2	453	471	4.0
2	2	573	574	0.2
3	3	611	612	0.2
3	2	800	810	1.3

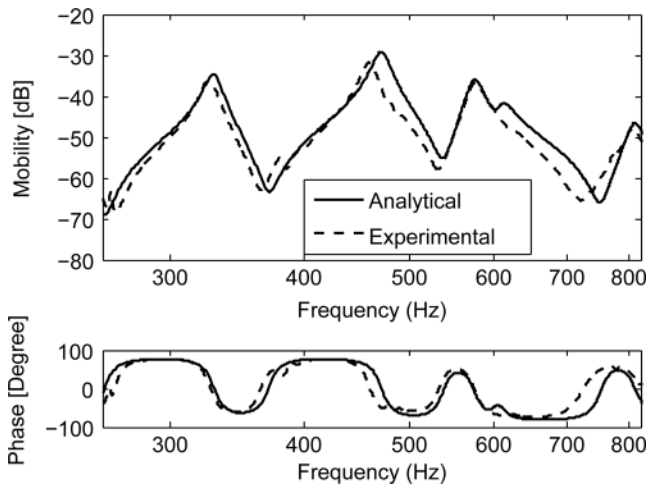


FIG. 3. Point mobility of the curved stiffened panel. Solid line, analytical result; dashed line, experimental result.

of the measured damping loss factors of the panel modes, 0.035. Figure 3 shows a comparison of the analytical and the measured point mobility. The solid curve is the predicted result using the smearing technique, and the dashed curve is the experimental result. Overall, a fairly good agreement can be seen, and the small deviations in mobility magnitude and phase reflect the deviations that were observed in the natural frequencies; this is especially the case for the 4% shift in the natural frequency of mode (1, 2) that results in about 5 dB deviation in the “mass-slope-region” of the mobility magnitude. From Fig. 3, it can also be observed that the weakly excited mode (3, 1) at 611 Hz is hardly visible in the measured result. This is because the drive point was relatively close to a nodal line of this mode; however, from an analysis of all measured data both its natural frequency and mode shape could be determined. Moreover, comparisons of predicted and measured responses at other positions also show a fairly good agreement with similar small deviations corresponding to those in the point mobility. This is seen in Fig. 4, which shows three examples of predicted and measured transfer mobilities for the response positions denoted as points 1–3 in Fig. 2. These points are located, respectively, in a plate field, on a stiffener, and at the crossing of two stiffeners; the location of stiffeners can be seen from the dashed lines in Fig. 2 that indicate the positions of the (hidden) stiffeners on the rear side of the panel.

An example of an experimentally determined modal pattern is shown in Fig. 5 in the form of a two-dimensional surface plot. The result shown is for mode (2, 1) at 327 Hz, and this clearly illustrates a modal pattern with two “half-sinusoidal” in the x direction and one half-sinusoidal in the y direction. This and the other mode shapes have been obtained from the real parts of the transfer mobilities measured at 192 positions, and the modal data have been normalized by the maximum amplitude value.

Two-dimensional plots are not suitable for comparing measured and predicted results. All the examined mode shapes are therefore shown in Fig. 6 by their detailed modal patterns in the x and y directions, respectively. The mode shapes predicted by the smearing technique are plotted as

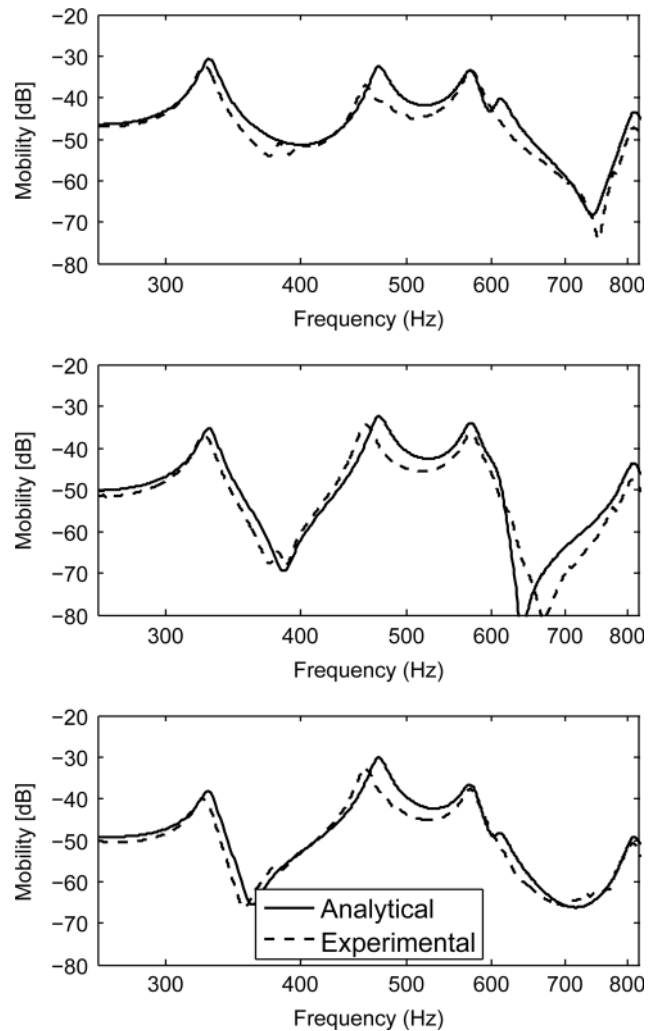


FIG. 4. Transfer mobility of the curved stiffened panel. Solid line, analytical result; dashed line, experimental result. The upper figure is the transfer mobility at point 1 in a plate field (see Fig. 2); the middle figure is at point 2 on a stiffener; the lower figure is at point 3 at the crossing of two stiffeners.

solid lines, whereas the experimentally determined mode shapes are presented as circles located at the actual measurement points; the dashed line represents the corresponding un-deformed panel surface-line. Overall the agreement is seen to be good between the predicted and measured results. A close inspection, however, reveals that there are small deviations. First, it is observed from the x -wise modal pattern of mode (2, 1) that there are small displacements at each end of the panel, and that these are in anti-phase. Similar observations can be made for modes (3, 1) and (3, 2). This is apparently caused by small shear deformations (displacements) at the experimental simple support, or by small motion of the whole experimental arrangement. Additional tests showed that the vibration level of the “rigid” frame were lower than the panel vibration by more than 25 dB at these modes. Thus, the edge-deviation is most likely caused by shear deformation at the narrow-strip support, which cannot fully accomplish an ideal simple line support. Second, it is observed that the measured modal patterns are not exactly sinusoidal as is the case for the predicted mode shapes; this applies in particular to mode (2, 2), both in the x and y

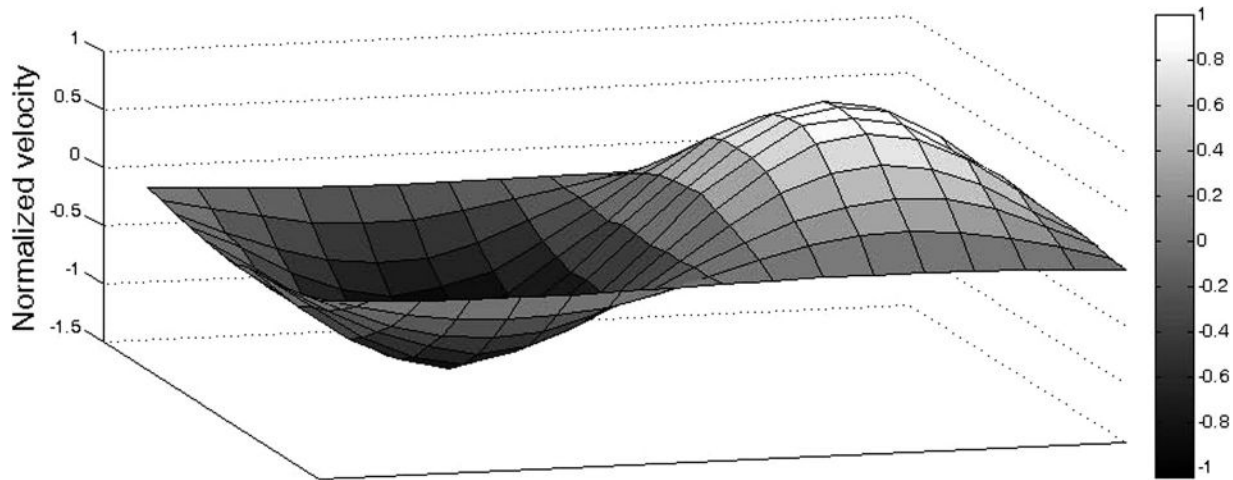


FIG. 5. Mode shape of mode (2, 1) obtained from experiment.

directions, and this causes the nodal lines to shift slightly from the predicted center positions of the zero-crossings. A possible explanation for this could be boundary vibration (albeit lower by 30 dB for this mode) of the supporting “rigid” frame and box structure or manufacturing inaccuracies in the curved stiffened panel; this was measured globally to be of the order of 1.5% for the thickness of the base panel, and this may have a small influence on the modal symmetry. The other modes, on the other hand, have mostly a fine match with the predicted modal patterns.

To sum up, the practically useable frequency range of the presented smearing technique is limited by the frequency at which half a bending wavelength in the base plate becomes comparable to—or smaller than—the stiffener spacing. This has been validated by the experiments reported herein, which have demonstrated that the prediction technique is reliable with an acceptable accuracy up to this frequency; at higher frequencies the technique may have a small influence on accurately replicating the actual mode shapes with beginning local deformation in base panel areas between adjacent stiffeners. However, this is outside the frequency range considered in this study. All in all, the prediction and the experiments have been found to be in good agreement, despite

the minor experimental difficulties that give rise to small unpredictable errors.

B. Radius study by numerical simulations

In Sec. IV A a weakly curved cross-stiffened panel was considered with curvature radii of $R_x = 2$ and $R_y = 1.5$ m. With the smearing technique experimentally validated for the considered modal range this section examines a new series of panels that are basically similar to the experimental structure but with different values of curvature radii R_x . In this simulation study the panel radius R_x takes values of 2.0, 1.5, 1.0, 0.6, and 0.2 m, whereas the other geometrical parameters are unchanged. Figure 7 shows the geometry of four of these models. In the lower part of the figure the panel is shown rotated so it is easier to see the arrangement of the stiffeners.

The natural frequencies of this series of curved cross-stiffened panels were computed analytically by the use of the smearing technique and, as a reference, corresponding detailed numerical FE analyses were carried out using the software package ANSYS. The element size used in the FE computations was set to be 10 mm, and the boundary conditions of the

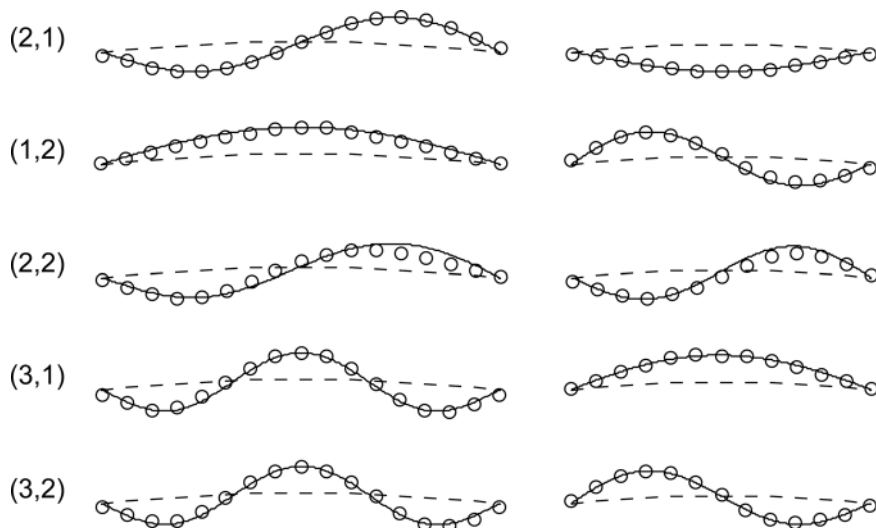


FIG. 6. Mode shape evaluation. The left-hand figures show the mode shapes in the x direction, while the right-hand figures are the mode shapes in the y direction. The corresponding mode numbers are shown to the left. Solid lines represent the theoretically determined mode shapes; the circles represent the experimentally determined mode shapes; and the dashed lines show the neutral positions of the curved base plate.

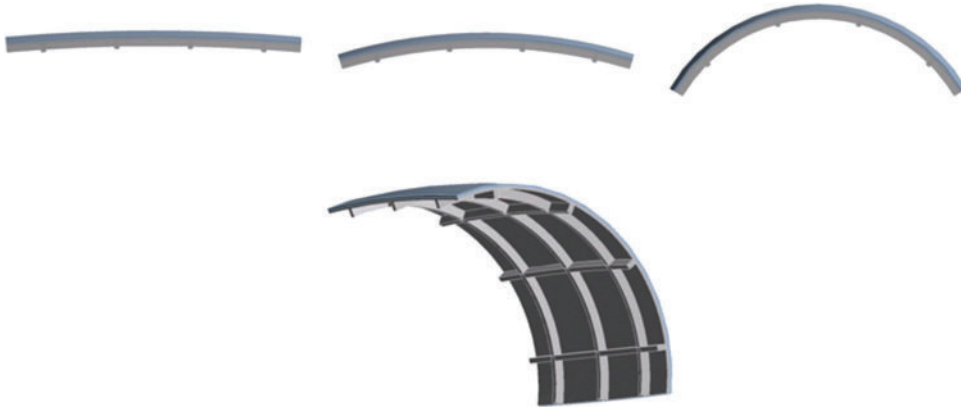


FIG. 7. (Color online) Geometries of four panel models. The upper models from left to right have a curvature radius R_x of 2.0, 1.0, and 0.6 m, respectively, while the lower model has a radius of $R_x = 0.2$ m.

models were again taken to be simply supported along the four panel edges.

The natural frequencies predicted with the analytical smearing technique ($f_{\text{analytical}}$) are compared with the results computed with the FE model (f_{FE}); the FE model contains all details of the structure and it is therefore considered to be the reference for evaluation of the prediction accuracy, as mentioned above. The deviation in predicted natural frequency is thus calculated as $100 \cdot (f_{\text{analytical}} - f_{\text{FE}}) / f_{\text{FE}}$, and the results for all modes are shown in Fig. 8. For each mode number n of an (m, n) mode the m values are connected by lines so that one can see how the error changes for different mode numbers m . It is observed that the deviations for all the modes shown are within -1% and $+4\%$ for curvature radii down to 0.6 m, and that the deviations become larger for the last model with smaller radius. Note that the fundamental mode (1, 1) is not included in this figure, since it is inaccurately predicted as mentioned in Sec. IV A. As an example, Fig. 9 shows the modal pattern of mode (2, 2) which is obtained from an FE simulation of the panel with

$R_x = 0.2$ m. It is obvious that the modal pattern is not sinusoidal but compressed by the two stiffeners close to the edges in the strongly curved direction. The developed method assumes that the mode shape is sinusoidal and therefore gives a large deviation for this mode as shown in Fig. 8. It indicates that the smearing technique for curved plate cannot be used for predicting accurate results for strongly curved plates. It can also be seen that the stiffeners are twisted by the base plate. Such local twisting cannot be predicted by the smearing theory since the stiffeners are smeared. All in all it may be summarized that for the current series of simulations, the natural frequencies are well predicted with the smearing technique even for panels of a relatively small radius of say 0.6 m.

V. CONCLUSIONS

A simple smearing method has been presented for calculating the natural frequencies, mode shapes, and forced vibrations of simply supported doubly curved and cross-stiffened thin rectangular shells. This developed smearing technique has been validated by experiments with a weakly doubly

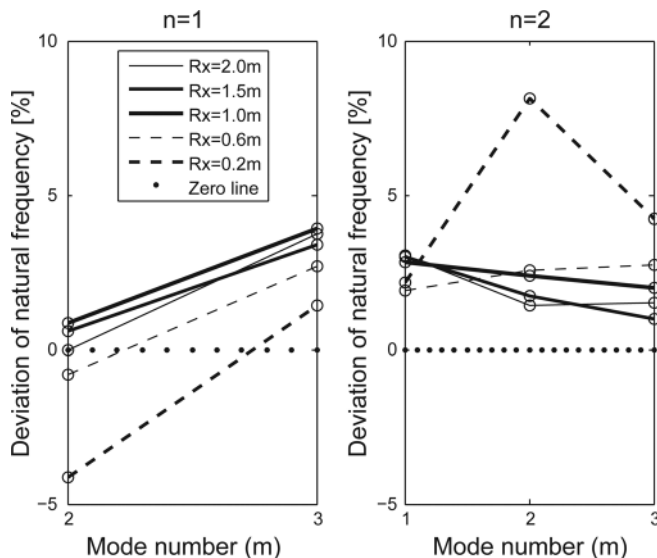


FIG. 8. Deviations of predicted natural frequencies for panels with different curvatures of radii of R_x . Natural frequencies obtained with the smearing technique ($f_{\text{analytical}}$) are compared with calculated results from the FE analysis (f_{FE}), which is considered as the reference. The deviation is calculated as $100 \cdot (f_{\text{analytical}} - f_{\text{FE}}) / f_{\text{FE}}$. The left-hand figure shows results for modes (2, 1) and (3, 1), while the right-hand figure is for modes (1, 2), (2, 2), and (3, 2).

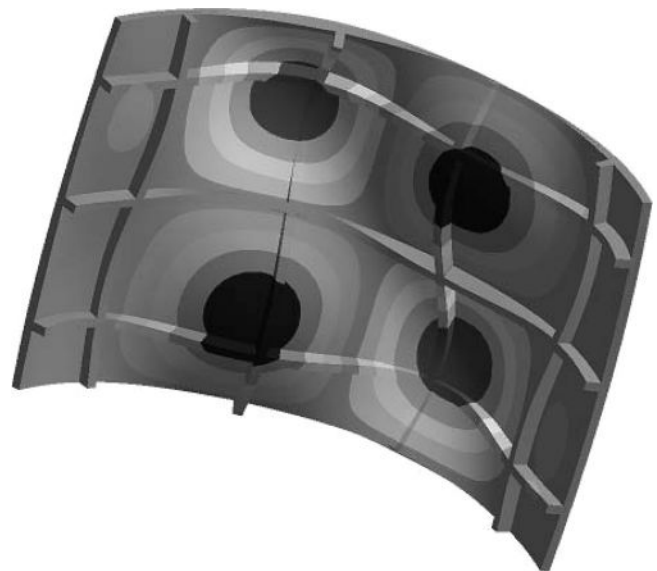


FIG. 9. Two-dimensional mode shape of mode (2, 2) obtained by the FE analysis for the panel with a curvature radius of $R_x = 0.2$ m and $R_y = 1.5$ m.

curved and cross-stiffened panel fabricated from a block of PVC-material. Comparison of the predicted and experimental results revealed a good agreement for the modal properties as well as for the forced panel responses. Simulation studies were also carried out for more curved panels by using the smearing technique and detailed FE analyses. For the cases examined herein, the results show that a reasonably good engineering accuracy can be obtained with limited computational effort for such doubly curved panels with moderate size cross-stiffeners.

This investigation also demonstrates that it is difficult to predict the fundamental panel mode (1, 1) of highly curved panels accurately when using the Donell–Mushtari–Vlasor’s shell equations. However, it is expected that it should be possible to improve the developed estimation method to a wider range of structures by adding a correction factor to these shell equations, as mentioned in Ref. 34.

APPENDIX: A BRIEF DESCRIPTION OF THE SMEARING TECHNIQUE FOR CROSS-STIFFENED THIN RECTANGULAR PLATE^{2,3}

The bending stiffness D_y can be calculated as the product of Young’s modulus of the material, E , and the area moment of inertia in the y direction, I_y , which is

$$I_y = I_p + I_{sy} + I_{sx}, \quad (\text{A1})$$

where the area moment of inertia of the plate with respect to the neutral axis of the system is

$$I_p = \frac{h^3}{12(1-\nu^2)} + \left(d_y - \frac{h}{2}\right)^2 \cdot h, \quad (\text{A2})$$

in which ν is the Poisson’s ratio, and d_y denotes the distance between the plate’s bottom surface and the neutral axis of the stiffened plate in the y direction. The area moment of inertia of the stiffeners with respect to the same neutral axis is

$$I_{sy} = \frac{1}{a_s} \cdot \left[\frac{w_{sy} \cdot h_{sy}^3}{12} + \left(h_{sy} + h - d_y - \frac{h_{sy}}{2}\right)^2 \cdot (w_{sy} \cdot h_{sy}) \right], \quad (\text{A3})$$

and, in the x direction,

$$I_{sx} = \frac{h_{ey}^3}{12} + h_{ey} \left(\frac{h_{ey}}{2} + h - d_y \right)^2. \quad (\text{A4})$$

The neutral axis d_y is

$$d_y = \frac{N}{D}, \quad (\text{A5})$$

with the numerator

$$N = \frac{1}{2} h^2 a_s b_s + a_s w_{sx} h_{sx} \left(h + \frac{h_{ey}}{2} \right) + b_s w_{sy} h_{sy} \left(h + \frac{h_{sy}}{2} \right) - w_{sx} w_{sy} \text{Min}\{h_{sx}, h_{sy}\} \left(h + \frac{\text{Min}\{h_{sx}, h_{sy}\}}{2} \right)$$

and the denominator

$$D = h a_s b_s + a_s w_{sx} h_{sx} + b_s w_{sy} h_{sy} - w_{sx} w_{sy} \text{Min}\{h_{sx}, h_{sy}\},$$

in which h_{ey} is the thickness of the added upper layer on the plate resulting from the smeared x stiffener. Note that the other geometrical parameters are defined in Fig. 1 in the main body of the paper.

The bending stiffness in the x direction, D_x , is obtained in a similar manner.

¹P. Lampert, “Postcracking stiffness of reinforced concrete beams in torsion and bending,” in *Analysis of Structural Systems for Torsion*, ACI SP-35, edited by R. Szilard, P. Zia, and G. Fisher (American Concrete Institute, Detroit, MI, 1973).

²R. Szilard, *Theories and Applications of Plate Analysis* (Wiley, Hoboken, NJ, 2004), Chap. 10.

³Y. Luan and M. Ohlrich, “An improvement of the smeared theory for stiffened plates,” in *Proceedings of Noise and Vibration: Emerging Methods 2009*, Oxford, England (2009).

⁴W. H. Hoppmann II, “Some characteristics of the flexural vibrations of orthogonally stiffened cylindrical shells,” *J. Acoust. Soc. Am.* **30**, 77–82 (1958).

⁵J. E. Manning, and G. Maidanik, “Radiation properties of cylindrical shells,” *J. Acoust. Soc. Am.* **36**, 1691–1698 (1964).

⁶S. A. Rinehart and J. T. S. Wang, “Vibration of simply supported cylindrical shells with longitudinal stiffeners,” *J. Sound Vib.* **24**, 151–163 (1972).

⁷D. J. Mead and N. S. Bardell, “Free vibration of a thin cylindrical shell with discrete axial stiffeners,” *J. Sound Vib.* **111**, 229–250 (1986).

⁸D. J. Mead and N. S. Bardell, “Free vibration of a thin cylindrical shell with periodic circumferential stiffeners,” *J. Sound Vib.* **115**, 499–520 (1987).

⁹B. A. J. Mustafa and R. Ali, “Prediction of natural frequency of vibration of stiffened cylindrical shells and orthogonally stiffened curved panels,” *J. Sound Vib.* **113**, 317–327 (1987).

¹⁰B. A. J. Mustafa and R. Ali, “Free vibration analysis of multi-symmetric stiffened shells,” *Comput. Struct.* **27**, 803–810 (1987).

¹¹N. S. Bardell and D. J. Mead, “Free vibration of an orthogonally stiffened cylindrical shell, part I: Discrete line simple supports,” *J. Sound Vib.* **134**, 29–54 (1989).

¹²N. S. Bardell and D. J. Mead, “Free vibration of an orthogonally stiffened cylindrical shell, part II: Discrete general stiffeners,” *J. Sound Vib.* **134**, 55–72 (1989).

¹³Z. Mecitoglu and M. C. Dokmeci, “Forced vibrations of stiffened cylindrical elastic panels (A),” *J. Acoust. Soc. Am.* **85**, S118 (1989).

¹⁴S. P. Cheng and C. Dade, “Dynamic analysis of stiffened plates and shells using spline Gauss collocation method,” *Comput. Struct.* **36**, 623–629 (1990).

¹⁵M. L. Accorsi and M. S. Bennett, “A finite element based method for the analysis of free wave propagation in stiffened cylinders,” *J. Sound Vib.* **148**, 279–292 (1991).

¹⁶Z. Mecitoglu and M. C. Dokmeci, “Free vibrations of a thin, stiffened, cylindrical shallow shell,” *AIAA J.* **30**, 848–850 (1991).

¹⁷R. S. Langley, “A dynamic stiffness technique for the vibration analysis of stiffened shell structures,” *J. Sound Vib.* **156**, 521–540 (1992).

¹⁸M. Conti and I. Dyer, “The influence of internal structures on bistatic scatter from finite cylindrical shells near axial incidence (A),” *J. Acoust. Soc. Am.* **94**, 1878 (1993).

¹⁹D. M. Photiadis, J. A. Bucaro, and B. H. Houston, “Scattering from flexural waves on a ribbed cylindrical shell,” *J. Acoust. Soc. Am.* **96**, 2785–2790 (1994).

²⁰G. Maze, D. Déculot, A. Klauson, and J. Metsaveer, “Acoustic scattering by immersed circular cylindrical shell stiffened by internal lengthwise rib (A),” *J. Acoust. Soc. Am.* **95**, 2868 (1994).

²¹A. Klauson, G. Maze, and J. Metsaveer, “Acoustic scattering by submerged cylindrical shell stiffened by an internal lengthwise rib,” *J. Acoust. Soc. Am.* **96**, 1575–1581 (1994).

²²A. Klauson, J. Metsaveer, D. Déculot, G. Maze, and J. Ripoché, “Identification of the resonances of a cylindrical shell stiffened by an internal lengthwise rib,” *J. Acoust. Soc. Am.* **100**, 3135–3143 (1996).

²³A. J. Stanley and N. Ganesan, “Free vibration characteristics of stiffened cylindrical shells,” *Comput. Struct.* **65**, 33–45 (1997).

²⁴D. M. Photiadis and B. H. Houston, “Anderson localization of vibration on a framed cylindrical shell,” *J. Acoust. Soc. Am.* **106**, 1377–1391 (1999).

- ²⁵M. H. Marcus, B. H. Houston, and D. M. Photiadis, "Wave localization on a submerged cylindrical shell with rib aperiodicity," *J. Acoust. Soc. Am.* **109**, 865–869 (2001).
- ²⁶M. Tran-Van-Nhieu, "Scattering from a ribbed finite cylindrical shell," *J. Acoust. Soc. Am.* **110**, 2858–2866(2001).
- ²⁷R. Liétard, D. Décultot, G. Maze, and M. Tran-Van-Nhieu, "Acoustic scattering from a finite cylindrical shell with evenly spaced stiffeners: Experimental investigation," *J. Acoust. Soc. Am.* **118**, 2142–2146 (2005).
- ²⁸D. G. Karczub, "Expressions for direct evaluation of wave number in cylindrical shell vibration studies using the Flügge equations of motion," *J. Acoust. Soc. Am.* **119**, 3553–3557 (2006).
- ²⁹M. Caresta and N. J. Kessissoglou, "Structural and acoustic responses of a fluid loaded cylindrical shell with structural discontinuities," *Appl. Acoust.* **70**, 954–963 (2009).
- ³⁰Z. Mecitoğlu, "Vibration characteristics of a stiffened conical shell," *J. Sound Vib.* **197**, 191–206 (1992).
- ³¹A. N. Nayak and J. N. Bandyopadhyay, "Dynamic response analysis of stiffened conoidal shells," *J. Sound Vib.* **291**, 1288–1297 (2006).
- ³²M. S. Troitsky, *Stiffened Plates* (Elsevier, Amsterdam, 1976), Chap. 8.
- ³³W. Soedel, *Vibrations of Shells and Plates*, 3rd ed. (Marcel Dekker, Inc., New York, 1993), Chap. 6.
- ³⁴L. Cremer, M. Heckl, and E. E. Ungar, *Structure-Borne Sound*, (Springer-Verlag, Berlin, 1988), Chap. 8, p. 186.